Flexural strengthening of RC beams with NSM CFRP laminates

Damian Szczech[1,*], *Łukasz* Krawczyk[1] and *Renata* Kotynia[1]

[1]Department of Concrete Structures, Lodz University of Technology, Poland

Abstract. The paper presents test results of reinforced concrete beams flexurally strengthened with Carbon Fibre Reinforced Polymer (CFRP) laminates using the Near Surface Mounted (NSM) technique. RC beams with a cross section of 200 x 400 mm were tested in four-point bending. Two RC beams were strengthened with one NSM CFRP laminate installed into the concrete cover on the bottom side of the beam. One of the beams was strengthened under the self-weight (B10.1) and the second one under initial preloading equal to 83% of the ultimate load of the reference beam (B10.1o). Failure mechanisms, cracking pattern and flexural behaviour of the beams are described in the paper. All the strengthened beams failed by rupture of the CFRP laminates followed by the internal steel reinforcement yielding. High strengthening efficiency of the NSM strengthening was confirmed by 109% and 130% when compared with the non-strengthened beam, respectively for beams B10.1 and B10.1o.

1 Introduction

Fibre reinforced polymer (FRP) materials are the best available alternative to conventional steel reinforcement, particularly with regard to the strengthening of reinforced concrete (RC) structures. This is due to being lightweight, non-corrosive, non-magnetic, high strength and with low thermal conductivity. FRP materials were introduced into civil engineering over fifty years ago [1, 2]. Research on flexural strengthening of RC structures with externally bonded (EB) FRPs indicated brittle failure due to FRP debonding and concrete cover delamination, as the most frequently observed failure modes. That confirms the tensile strength of the FRP materials cannot be utilized. Efficiency of the EB FRP reinforcement strongly depends on failure modes which is below 15% of the tensile strength for the end peeling of the FRP and about 35 ÷ 45% of the tensile strength for the midspan debonding of the FRP [3]. In the EB configuration, FRP laminates and sheets are bonded to the surface of the structural element, which makes them susceptible to damage from collision, severe environmental conditions like ultraviolet radiation, moisture absorption, high temperature and fire. These agents may reduce the service life of RC structures.

* Corresponding author: damian.szczech@p.lodz.pl

In order to avoid these drawbacks, the near surface mounted (NSM) technique was introduced, particularly in bridge structures [4-7]. This is a promising technology for increasing the flexural and shear capacity of deficient reinforced concrete members.

In the NSM FRP strengthening configuration, strips or bars are bonded into longitudinal grooves cut in the concrete cover located in the tensile region of the RC member, which mitigates the risk of abrupt FRP debonding from the concrete substrate. Recent studies on the NSM FRP reinforcement used for flexural strengthening of RC structures confirmed it as significantly more efficient comparing to the EB configuration. In fact, the reason of this benefit is much improved FRP-to-concrete bond behaviour of the NSM versus the EB technique caused by superior anchorage in adjacent concrete cover. The NSM FRP anchoring in the concrete component made this technique applicable in the negative bending moment regions, where the EB FRP reinforcement is exposed to mechanical failure. Application of NSM strips is more efficient than NSM bars because it increases contact surface between the composite and concrete but requires a thicker concrete cover. In fact, the choice of the specific type of the FRP material in flexural strengthening of RC members depends mainly on the concrete's thickness and the required FRP reinforcement ratio.

The NSM FRP technique provides improved fire resistance when compared with the EBR FRP one. However, the employment of a higher glass temperature epoxy has the strongest impact for NSM FRP applications in the internal structural RC members requiring high fire resistance. A state of the art in the field of flexural strengthening of RC members with the NSM FRP reinforcement based on hitherto experimental test results on the NSM technique indicated a significant increase in the load bearing capacity and the FRP tensile strain utilization of up to 80 % in comparison to EB FRP applications [8-10].

The application of FRP strips with higher height than the concrete cover thickness leads to a potential risk of cutting the main reinforcement. Furthermore, flexural strengthening using NSM rectangular strips is limited by the initial deflections of the RC member and cannot guarantee sufficient bond conditions.

The effects of several parameters such as geometry, steel and FRP reinforcement ratio, elasticity modulus of FRP reinforcement, concrete strength and a depth of the FRP reinforcement were published in terms of the failure modes, strengthening efficiency and FRP strain utilization [11, 12]. The observed failure modes contained: concrete crushing, FRP debonding with delamination of concrete cover, concrete-epoxy interface failure and FRP rupture [7, 13, 14-20].

2 Experimental program

2.1 Test specimens

The paper presents test results of a part of an extensive research program. Three single-span reinforced concrete beams with a cross section of 200 × 400 mm and a span of 3600 mm were tested under four-point loading. The tensile and compressive reinforcement consisted of two steel bars of 10 mm diameter (ρ_l = 0.216%). Vertical stirrups of 6 mm diameter were applied over the full shear span (a = 210 mm) at a spacing of 150 mm. The concrete cover of the main reinforcement was 31 mm. The static scheme of the beams with geometry and reinforcement details is shown in Table 1 and Fig. 1.

Table 1. Specimen details.

Element	Tensile reinforcement	Strengthening	Preloading
B10	2 ϕ 10 ρ_l = 0.216%	-	-
B10.1		1 CFRP strip	self-weight of the beam
B10.1o		1 CFRP strip	83% of the non-strengthened beam

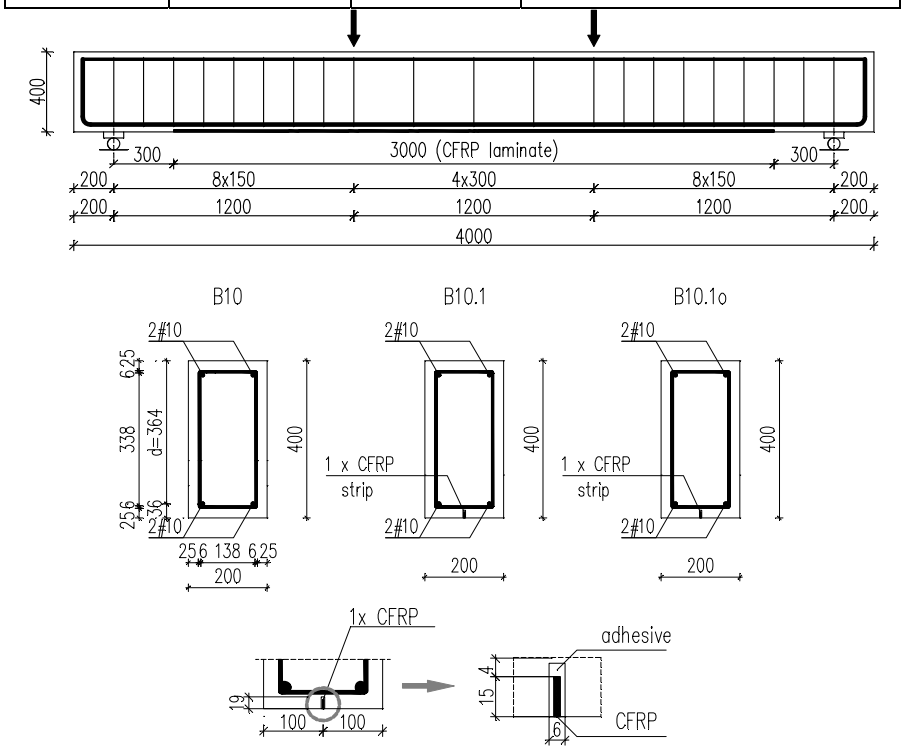

Fig. 1. Geometry of beams with internal reinforcement and strengthening configuration.

2.2 Concept of strengthening

The beams were strengthened with one CFRP laminate of 2.5 mm × 15 mm cross section bonded into a groove cut in the concrete cover of 6 mm × 19 mm cross section with the epoxy adhesive over the length of 3000 mm from the centre of beams. One of the RC beams (reference beam) was tested without any strengthening. Two beams: B10.1 and B10.1o, were strengthened under self-weight and under 83% of the ultimate load capacity of non-strengthened beam, respectively. The details of strengthening are presented in Fig. 2.

Fig. 2. Strengthening with NSM CFRP strips.

2.3 Material characteristics

The beams were casted with the concrete class C40/50. The mean strength of concrete ($f_{c,cube}$, $f_{c,cyl}$ - compressive cubic and cylinder concrete strength, respectively; $f_{ct,sp}$ - tensile concrete strength by splitting; E_c - elasticity modulus of concrete) is shown in Table 2.
The steel bars of RB500W class were used for the internal reinforcement. The mean strength of this reinforcement (f_{sy} - yield strength; f_{su} - tensile strength; E_s - elasticity modulus) is shown in Table 3.
The CFRP laminate CFK-Lamellen S&P was used for the beams' strengthening. Fully elastic behaviour was confirmed in the tensile test of the CFRP strips. The mean strength characteristic (f_{fu} - tensile strength; E_s - elasticity modulus) is shown in Table 4.

Table 2. Properties of concrete.

Element	$f_{c,cube}$ [MPa]	$f_{ct,sp}$ [MPa]	$f_{c,cyl}$ [MPa]	E_c [GPa]
B10, B10.1, B10.1o	53.3	3.6	42.0	31.1

Table 3. Mechanical properties of steel reinforcement.

Reinforcement	Diameter [mm]	f_{sy} [MPa]	f_u [MPa]	E_s [GPa]
Steel bars	6	656.0	687.5	200
	10	529.4	628.3	202

Table 4. Mechanical properties of CFRP laminates.

Strengthening material	Geometry $b_f \times h_f$ [mm]	f_{fu} [MPa]	E_f [GPa]
CFRP laminate	15 × 25	2520	168

2.4 Test setup and measurements

The beams were tested in a test setup composed of steel frame structure, a hydraulic jack attached to the upper part of the frame and steel hinged supports (one movable). The beam was loaded gradually until failure. The measuring device consisted of several linear variable differential transducers (LVDT) and strain gauges. For concrete strain measurements, LVDT gauges were located on the lateral surface of the beam at the compressive and tensile steel reinforcement levels (Fig. 3). Additional LVDTs were applied along the entire length of beams for deflection measurements. Strain gauges were installed on the CFRP strips (Fig. 4).

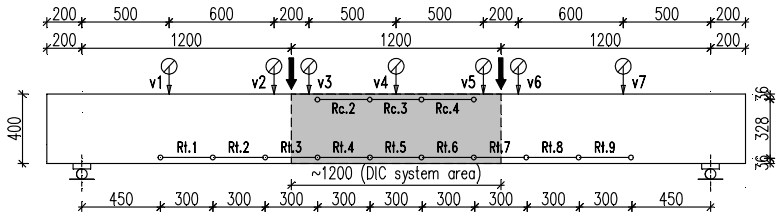

Fig. 3. Scheme of concrete strain and deflection measurements.

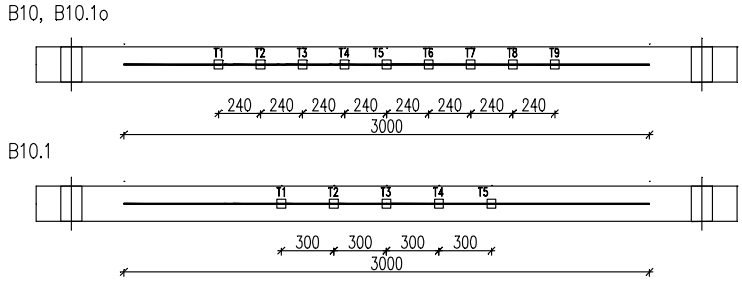

Fig. 4. Scheme of CFRP strain measurements (strain gauges).

Moreover, during experimental tests of beams B10 and B10.1o Digital Image Correlation (DIC) system [21] was used to collect data of the concrete surface deformations. The displacements of concrete points in the central part of each element were registered with the DIC photos (marked in Fig. 3). The central part of the beam was painted white and sprayed with black dots. These actions made contrast suitable to allow the DIC find facets necessary for making measurements [22, 23]. The deflections of B10 and B10.1o beams were registered in points v3, v4 and v5, corresponding to the LVDT gauges (see Fig. 3). Additionally, concrete strain was measured in the constant bending moment on the virtual basis to compare them with LVDTs (marked Rc.2, Rc.3, Rc.4, Rt.4, Rt.5 and Rt.6, Fig. 4).

3 Analysis of test results

3.1 Experimental observations

Comparison between vertical displacement, average concrete strain and curvature of tested beams is shown in Figs. 5÷8. All curves are similar up until the load of 18 kN, which corresponds with the uncracked range. For higher load values, a significant difference between B10 beam and two strengthened elements was registered. For beam B10, steel reinforcement yielding started under the load of 23 kN, while in beams B10.1 and B10.1o the load increased linearly up to failure. However, deflections of both strengthened beams are generally similar.

The vertical displacements for both strengthened beams under the self-weight (B10.1) and under the preliminary load (B10.1o) are almost the same for the higher loads. The average concrete strain along the pure bending region is very similar for both strengthened elements (Fig. 5) and similar to the curvature of beams (Fig. 6 and Fig. 7).

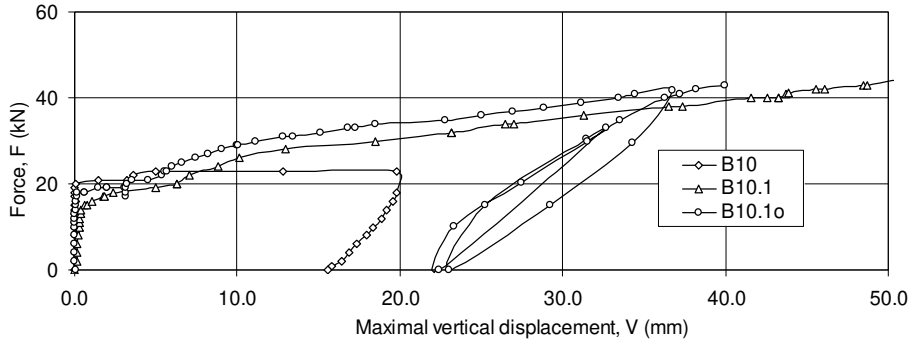

Fig. 5. Vertical displacement.

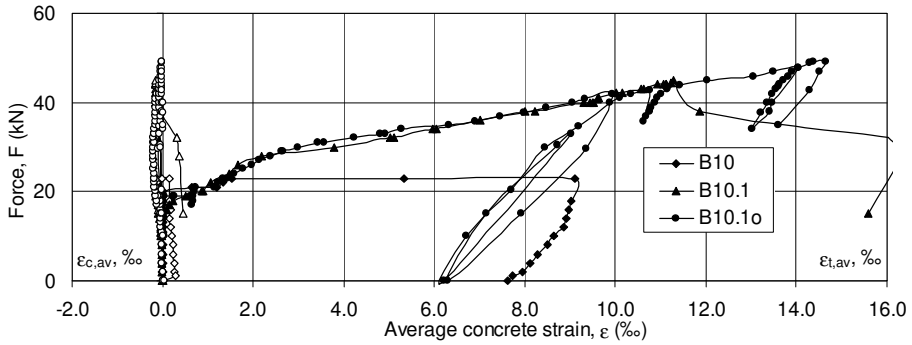

Fig. 6. Average concrete strain measurements.

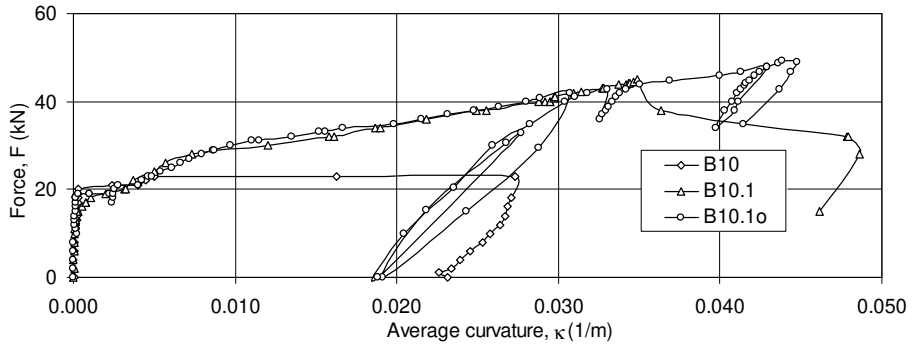

Fig. 7. Average curvature.

Strains of CFRP strips for strengthened elements are compared in Fig. 8. The first observation is that curves for both elements are parallel to each other. The main difference between both curves based on the preloading level during the beams strengthening (self-weight for B10.1 beam and self-weight with external load of 19 kN for B10.1o beam). It is clearly visible that the strengthening of beam B10.1o under higher preloading level made the beam stiffer after cracking by the crack bonding with the adhesive. This is why the beam strengthened under self-weight indicated higher strain values for the same load levels as the beam strengthened under external load.

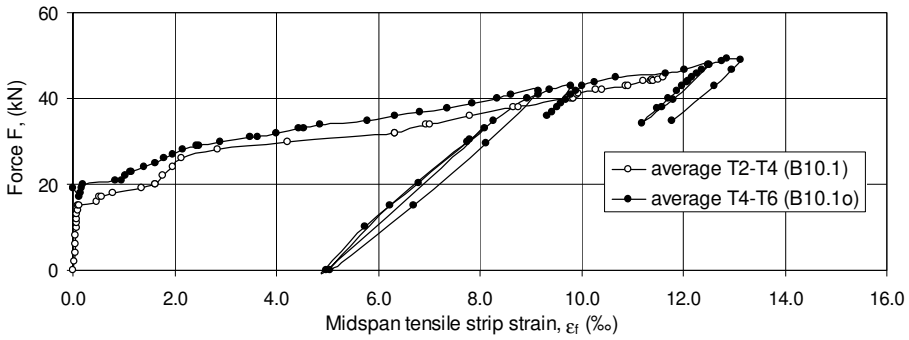

Fig. 8. Average CFRP strains measured along the pure bending region.

Comparison of average curvature based on concrete strains registered by the DIC and LVDT gauges (Fig. 9) confirms very good compatibility between both techniques of measurements.

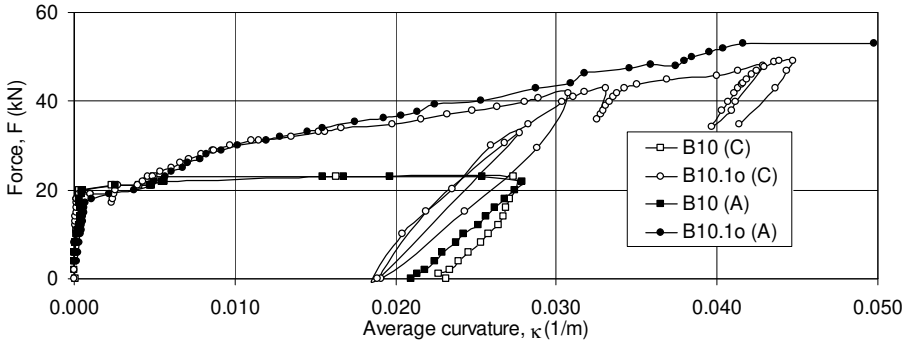

Fig. 9. Average curvature based on: LVDT gauges (C) and Aramis DIC system (A).

The same results confirm deflections registered for the strengthened beams with both techniques (see Fig. 10).

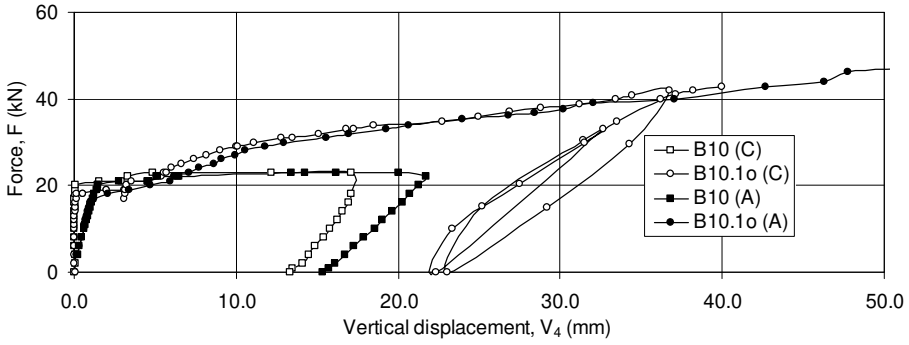

Fig. 10. Vertical displacement based on: LVDTs sensors (C) and Aramis DIC system (A).

3.2 Cracking and failure mode

The crack development registered in the beams shows classical flexural cracking with the vertical cracks in the pure bending region, which developed towards the top surface of the

beams as the load increased. The cracking pattern in both strengthened elements showed a similar character (Fig. 11 – Fig. 13). The first primary crack was formed at the point of concentrated force loading. These primary flexural cracks developed in the stirrup locations. Then another crack was created in the middle of the span of the members and another one under the second concentrated force. Subsequently, small cracks developed as secondary bending cracks located between two adjacent primary cracks. The scratch developed symmetrically in relation to the middle of the span of the elements. In the strengthened beams, bending cracks branched off near the bottom edge of beams. The crack patterns of all beams consisted predominantly of flexural cracks.

All the strengthened beams failed by the rupture of the CFRP laminate after the yielding of the tension steel reinforcement. The failure was sudden and brittle, accompanied by the crackle of bursting CFRP laminate. After the concrete cover was removed, longitudinal cracks were visible on the strip, usually in the middle of its height. The maximum strain values of the CFRP laminate obtained in the middle of the strip length were equal to 12‰.

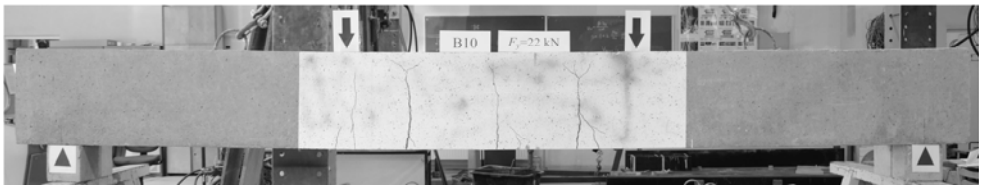

Fig. 11. Failure of beam B10.

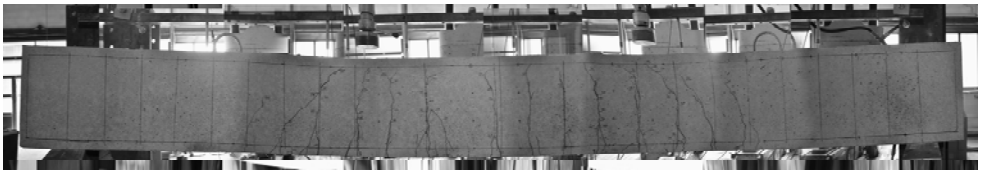

Fig. 12. Failure of beam B10.1.

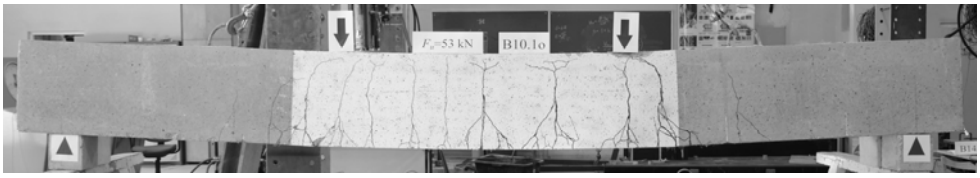

Fig. 13. Failure of beam B10.1o.

3.3 Experimental results

The most important result of the research is the potential to increase the load bearing capacity of strengthened beams by more than 100% compared to an unstrengthened one. The test results are summarized in Table 5. Based on the observation of the beams and the tensile concrete strain measurements, all tested beams confirmed flexural cracking under the load of about 18 kN.

The reference beam without any strengthening (B10) failed at an ultimate load equal to 23 kN. Strengthening the beam with one CFRP laminate under self-weight (B10.1) caused a 109% increase in the ultimate load capacity in comparison with the non-strengthened one. In the case of beam B10.1o, strengthened under an external load of 19 kN, the flexural capacity increased by 10% in comparison with beam B10.1, and it reached almost 130% of the ultimate capacity of the unstrengthened beam.

Table 5. Test results.

Element	Cracking load	Strengthening external load	Ultimate load	Strengthening ratio
	[kN]	[kN]	[kN]	[-]
B10	19	---	23	---
B10.1	18	0	48	2.09
B10.1o	18	19	53	2.30

4 Conclusions

The paper presents the test results of reinforced concrete beams flexurally strengthened with CFRP laminates using the NSM technique. Experimental tests carried out on concrete beams enabled the following conclusions to be drawn:

1) Ultimate load for both strengthened beams is more than 100% higher than for the unstrengthened one.
2) A negative effect of extensive preloading on the strengthening efficiency was not observed. The beam strengthened after preloading equal to 83% of the ultimate load of the non-strengthened beam resisted 9% higher load than the beam strengthened under self-weight.
3) Deflections and the strains of the CFRP strip are lower for the initially preloaded beam than for the beam not preloaded.
4) The measurements made by LVDT gauges and the DIC offered very compatible results.

References

1. U. Meier, M. Deuring, H. Meier, G. Schwegler. Strengthening of Structures with CFRP Laminates: Research and Applications in Switzerland, Proc. of the Advanced Composite Materials in Bridges and Structures, CSCE, 243-251, Sherbrooke (1995).
2. J. G. Teng, S. Smith, FRP-Strengthened RC Beams. I: Review of Debonding Strength Models, Eng. Struct. **24**, 385–395 (2002).
3. R. Kotynia, H. Abdel Baky, K. Neale, U. Ebead. Flexural strengthening of RC beams with externally bonded CFRP systems: test results and 3-D nonlinear FE analysis, Journal of Composites for Construction, ASCE, **12**, 2, 190-201 (2008).
4. M. Blaschko. Zum Tragverhalten von Betonbauteilen mit in Schlitze eingeklebten CFK-Lamellen, Ph.D. Dissertation, Technische Univeritat Munchen, **187**, (2001).
5. H. Nordin, B. Täljsten, A. Carolin, Concrete beams strengthened with prestressed near surface mounted reinforcement. Proc. of the International Conference on FRP Composites in Civil Engineering, Hong Kong, China, 1067-1075 (2001).
6. R. El-Hacha, S. Rizkalla, Near-surface-mounted fiber-reinforced polymer reinforcements for flexural strengthening of concrete structures, Struct. J. **101**, (2004).
7. R. Kotynia, Analysis of reinforced concrete beams strengthened with near surface mounted FRP reinforcement. Arch. Civil. Mech. Eng. **LII**, 2, 305–17 (2006).

8. B. Täljsten, A. Carolin, H. Nordin, Concrete structures strengthened with near surface mounted reinforcement of CFRP, Adv. Struct. Eng. **6**, 3, 201–13 (2003).
9. J. Barros, R. Kotynia, Possibilities and challenges of NSM for the flexural strengthening of RC structures, Proc. of Fourth International Conference on FRP Composites in Civil Engineering CICE2008, Zurich, Switzerland. (2008).
10. L. De Lorenzis, J. Teng, Near-surface mounted FRP reinforcement: An emerging technique for strengthening structures, Compos. Part B **38**, 119–143 (2007).
11. J. Teng, L. De Lorenzis, B. Wang, R. Li, T. Wong, L. Lam, Debonding failures of RC beams strengthened with near surface mounted CFRP strips, J. Compos. Constr. **10**, 2, (2006).
12. H. Rasheed, R. Harrison, R. Peterman, T. Alkhrdaji, Ductile strengthening using externally bonded and near surface mounted composite systems, Compos. Struct. **92**, (2010).
13. J. Yost, S. Gross, D. Dinehart, J. Mildenberg, Flexural behaviour of concrete beams strengthened with near-surface-mounted CFRP strips, ACI Struct. J. **104**, 4, (2007).
14. A. Astorga, H. Santa Maria, M. Lopez, Behavior of a concrete bridge cantilevered slab reinforced using NSM CFRP strips, Constr. Build. Mater. **40**, 461–472 (2013).
15. J. Barros, S. Dias, J. Lima, Efficacy of CFRP-based techniques for the flexural and shear strengthening of concrete beams, Cem. Concr. Compos. **29**, (2007).
16. F. Al-Mahmoud, A. Castel, R. François, C. Tourneur, Strengthening of RC members with near-surface mounted CFRP rods, Compos. Struct., **91**, 138–147 (2009).
17. S. Soliman, M. El-Salakawy, B. Benmokrane, Flexural behaviour of concrete beams strengthened with near surface mounted fibre reinforced polymer bars, Can. J. Civ. Eng. **37**, 10, 1371-1382 (2010).
18. fib Bulletin 90. Externally applied FRP reinforcement for concrete structures. Technical report prepared by a working party of the T5.1 FRP reinforcement for concrete structures. Co-author chapters: 5. Bond and 6. Ultimate limit states for predominantly static loading and fatigue. (2019).
19. R. Kotynia. FRP Composites for Flexural Strengthening of Concrete Structures. Theory, Testing, Design. Lodz University of Technology Press. ISBN 978-83-7283-996-1. pp. 240. (2019).
20. R. Kotynia, M. Przygocka, Preloading effect on strengthening efficiency of RC beams strengthened with non- and pretensioned NSM strips, Polymers **10**, 2, (2018).
21. Digital Image Correlation and Strain Computation Basics, GOM Testing Technical Documentation as of V8 SR1.
22. Ł. Krawczyk, Strengthening of short corbels with embedded through-section reinforcement (in polish) Doctoral Thesis Lodz University of Technology, (2017).
23. Ł. Krawczyk, M. Gołdyn, T. Urban, Digital Image Correlation Systems in the Experimental Investigations: Capabilities and Limitations, Arch. Civ. Eng. **65**, 1, (2019).